



HAL
open science

Myriophyllum alterniflorum biochemical changes during in vitro Cu/Cd metal stress: Focusing on cell detoxifying enzymes

Raphael Decou, David Delmail, Pascal Labrousse

► To cite this version:

Raphael Decou, David Delmail, Pascal Labrousse. Myriophyllum alterniflorum biochemical changes during in vitro Cu/Cd metal stress: Focusing on cell detoxifying enzymes. Aquatic Toxicology, 2020, 219, pp.105361. 10.1016/j.aquatox.2019.105361 . insu-02371690

HAL Id: insu-02371690

<https://insu.hal.science/insu-02371690>

Submitted on 20 Nov 2019

HAL is a multi-disciplinary open access archive for the deposit and dissemination of scientific research documents, whether they are published or not. The documents may come from teaching and research institutions in France or abroad, or from public or private research centers.

L'archive ouverte pluridisciplinaire **HAL**, est destinée au dépôt et à la diffusion de documents scientifiques de niveau recherche, publiés ou non, émanant des établissements d'enseignement et de recherche français ou étrangers, des laboratoires publics ou privés.

Journal Pre-proof

Myriophyllum alterniflorum biochemical changes during *in vitro* Cu/Cd metal stress: Focusing on cell detoxifying enzymes

Raphaël Decou, David Delmail, Pascal Labrousse



PII: S0166-445X(19)30527-2
DOI: <https://doi.org/10.1016/j.aquatox.2019.105361>
Reference: AQTOX 105361

To appear in: *Aquatic Toxicology*

Received Date: 4 July 2019
Revised Date: 14 November 2019
Accepted Date: 14 November 2019

Please cite this article as: Raphaël D, David D, Pascal L, *Myriophyllum alterniflorum* biochemical changes during *in vitro* Cu/Cd metal stress: Focusing on cell detoxifying enzymes, *Aquatic Toxicology* (2019), doi: <https://doi.org/10.1016/j.aquatox.2019.105361>

This is a PDF file of an article that has undergone enhancements after acceptance, such as the addition of a cover page and metadata, and formatting for readability, but it is not yet the definitive version of record. This version will undergo additional copyediting, typesetting and review before it is published in its final form, but we are providing this version to give early visibility of the article. Please note that, during the production process, errors may be discovered which could affect the content, and all legal disclaimers that apply to the journal pertain.

© 2019 Published by Elsevier.

***Myriophyllum alterniflorum* biochemical changes during *in vitro* Cu/Cd metal stress:**

Focusing on cell detoxifying enzymes

Short title: Watermilfoil antioxidant enzyme activities in response to *in vitro* metal stress

Raphaël DECOU^{a*}, David DELMAIL^{ab} and Pascal LABROUSSE^a

^a University of Limoges, PEIRENE, EA 7500, F-87000 Limoges, France

^b University of Rennes 1, UMR 6118 Géosciences, F-35043 Rennes, France

***Corresponding author:**

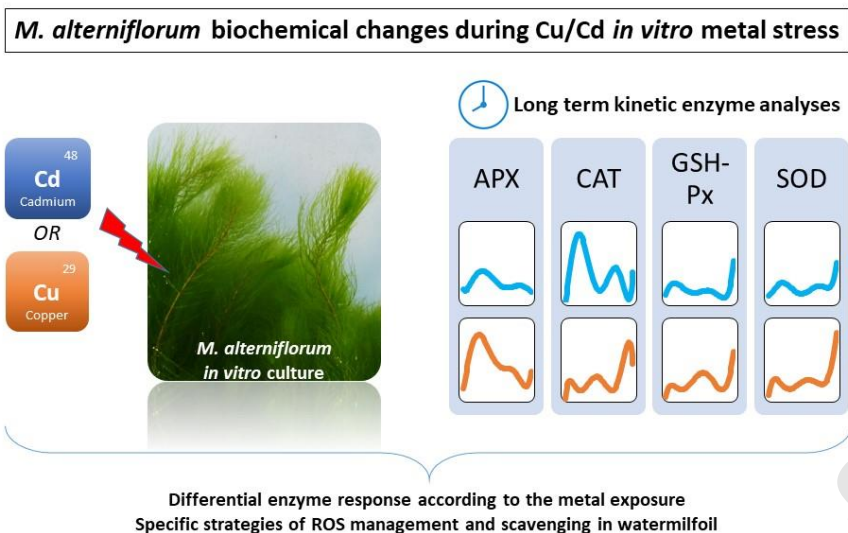
raphaeldecou@yahoo.fr or raphael.decou@unilim.fr

Laboratoire de Botanique et Cryptogamie - PEIRENE EA 7500

Faculté de Pharmacie, 2 rue du Dr. Marcland, 87025 Limoges Cedex, France

Phone: +33 (0)5 55 435 841

Graphical abstract



Highlights

- Respectively, APX and CAT strongly and quickly respond to Cu and Cd stresses
- At the contrary, SOD and GSH-Px were less enlisted for watermilfoil ROS scavenging
- Trace metal concentrations influenced the temporality of the enzyme involvements
- High concentration of copper suggested an oxidative stress limited by ion competition
- Overall data highlighted specific strategies of ROS management in watermilfoil

ABSTRACT

Given the toxicity of trace metals, their concentration, speciation and bioavailability serve to induce various plant detoxification processes, which themselves are specific to several parameters like plant species, tissue type and developmental stage. In this study, *Myriophyllum alterniflorum* (or alternate watermilfoil) enzyme activities (ascorbate peroxidase, catalase, glutathione peroxidase and superoxide dismutase) from *in vitro* cultures was measured over 27 days in response to copper (Cu) or cadmium (Cd) stress. These enzymes are unique to reactive oxygen species (ROS) scavenging (mainly hydrogen peroxide H_2O_2 and superoxide anion $\text{O}_2^{\bullet-}$) and moreover showed specific or unspecific activity

profiles, depending on the metal concentrations used. Our results suggest a higher-priority protection of chloroplasts during the initial days of exposure to both metals. At the same time, the increased catalase activity could indicate an H_2O_2 diffusion in peroxisome in order to protect other organelles from ROS accumulation. However, as opposed to the Cd effects, high Cu concentrations appear to induce a “limited oxidative threshold” for some antioxidant enzymes, which could suggest an ion absorption competition between Cu^{2+} and Fe^{2+} . In spite of an overall analysis conducted of the scavenging processes occurring in plant cells, biochemical analyses still yielded relevant indications regarding the watermilfoil strategies used for ROS management.

KEYWORDS: Aquatic plant; Reactive oxygen species; Antioxidant enzymes; Trace metals; Oxidative stress, *In vitro*.

1. Introduction

Reactive oxygen species (ROS) production and scavenging processes are common characteristics of cells. These toxic molecules are derived from successive one-electron reductions of molecular oxygen (O_2) and comprise a variety of forms, including superoxide radicals ($O_2^{\bullet-}$), hydrogen peroxide (H_2O_2), singlet oxygen (1O_2), hydroxyl radical ($\bullet OH$), perhydroxyl radical ($HO_2\bullet$) and alkoxy radicals ($RO\bullet$) (Bolwell and Wojtaszek, 1997; Gill and Tuteja, 2010; Delmail and Labrousse, 2012; Mullineaux *et al.*, 2018). Despite their significant role in plant growth and development [by virtue of their use as an oxidant for cell wall cross-linking, cell wall-loosening and as a signaling molecule controlling various biological processes (Kärkönen and Kuchitsu, 2015)], ROS also serve as warning signals tied to intracellular degradation processes in plants. Being generated at the basal level under favorable conditions, the ROS balance between ROS production and ROS scavenging

actually avoids all plant cell damage (Das and Roychoudhury, 2014). In contrast, the imbalance caused by stresses, such as trace metals, induces an oxidative stress capable of leading to cell death. To prevent this ultimate outcome and cope with environmental disturbances, the cell machinery implements the ROS beforehand in order to modify metabolism and genic expressions (Gill and Tuteja, 2010).

To counteract the hyperaccumulation of ROS in cells and to guarantee a metal tolerance capacity, plants have developed various systems that mainly include a series of chelating molecules and antioxidant enzymes. On the one hand, these chelating molecules are highly represented by reduced glutathione (GSH, corresponding to the tripeptide γ -glutamyl-cysteinyl-glycine), phytochelatin (PC, heavy metal-binding peptides derived from GSH), proline, α -tocopherol (lipophilic antioxidant), carotenoids and ascorbic acid (the most abundant antioxidant and contributor to the cellular redox state). Whereas on the other hand, antioxidant enzymes are primarily composed of ascorbate peroxidase (APX), catalase (CAT), glutathione peroxidase (GSH-Px) and superoxide dismutase (SOD), each of which presents its own activity and specificity. As a matter of fact, APX is a major H_2O_2 detoxifying system in plant cells and moreover catalyzes the conversion of H_2O_2 into H_2O by the use of ascorbate as a specific electron donor. CAT, also a heme-detoxifying enzyme (tetrameric), catalyzes the dismutation reaction of H_2O_2 into H_2O without any reductant (this enzyme is an efficient ROS scavenger since it can dismutate approx. 6 million molecules of H_2O_2 per minute; Gill and Tuteja, 2010). Glutathione peroxidase is another H_2O_2 -scavenging (but non-heme) enzyme, while SOD is a metalloprotein participating in plant stress tolerance through catalyzing the dismutation of $O_2^{\bullet-}$ into molecular oxygen and H_2O_2 . Other enzymes, such as monodehydroascorbate reductase, dehydroascorbate reductase, glutathione reductase (GR), glutathione-S-transferase, guaiacol peroxidase and peroxidase, also participate to a great extent in cell detoxification during ROS release (Gill and Tuteja, 2010; Mittler *et al.*, 2004).

These enzymes therefore work in concert and feature a subcellular location, dependent on their chemical specificities, in order to maintain the redox homeostasis. In addition, they possess a number of isoforms that are in shared organelles, cytosol and apoplast; as an example, CAT shows up for a predominant localization in peroxisomes while APX occurs mostly in chloroplasts and mitochondria but also in cytosol and peroxisomes (Anjum *et al.*, 2016). SOD and GSH-Px are present in all cellular compartments, e.g. chloroplasts, mitochondria, nucleus, peroxisomes, cytosol and apoplast (Gill and Tuteja, 2010; Alscher *et al.*, 2002; Gill *et al.*, 2015).

Despite all these advantages in terms of cell localization and specificity, enzyme activity differs during metal/metalloid stresses according to plant species, tissue type and plant age/developmental stage (Anjum *et al.*, 2016). Consequently, it becomes nearly impossible to extrapolate results from one plant species to another, thus complicating the understanding of cell detoxification mechanisms.

In macrophytes, only limited biochemical data on plants exposed to metal stress are available although these (hyper)accumulator plants are highly used for phytoremediation studies dealing with the surface-water quality and/or on wastewater treatments (Newete and Byrne, 2016). In keeping with our previous studies focusing on developmental and physiological approaches (Delmail *et al.*, 2011a, b) and to better understand the strategy of ROS scavenging in aquatic plants during Cu or Cd exposure, we therefore specifically analyzed, in the submerged macrophyte *Myriophyllum alterniflorum* (watermilfoil), the biochemical activity of four antioxidant enzymes frequently used as bioindicators of water pollutions (Gao *et al.*, 2019; Harguinteguy *et al.*, 2019). This native species in Europe is highly observed in aquatic ecosystem of the Limousin Region (France) and is resilient to metal pollutants that allows it to uptake and remove these contaminants from water and sediments of rivers (Delmail *et al.*, 2013). Moreover, for a better evaluation of these enzyme activity changes during the ROS

management mechanisms, trace elements were introduced at different concentrations.

Although the results obtained cannot be applied to field plants, given that the experiments were performed on *in vitro* watermilfoil cultures, this study will still provide preliminary data of potential use in subsequent *in situ* studies. Aquatic plants are being envisaged as biological indicators of the ecological state of freshwater (Harguinteguy *et al.*, 2013, 2016, 2019; Decou *et al.*, 2018, 2019) in the same way as fishes, invertebrates or mollusks. As such, this study aims to answer the three following questions: (i) is an enzymatic antioxidant system activated during a sequential burst in response to trace-metal exposure? (ii) is this response dependent on both the trace metal and concentration applied? (iii) are these enzymatic parameters potentially usable for *in situ* monitoring?

2. Materials and methods

2.1 Plant material

A *M. alterniflorum* clone, collected in the Vienne River, was disinfected and then transferred into sterile Murashige & Skoog's medium (1962) adjusted to pH 6.8 before autoclaving and supplementing with 3% sucrose. During the micropropagation process, the plant clones were maintained in a growth cabinet set at $24 \pm 2^\circ\text{C}$, with a photoperiod of 16 h and a light intensity of $7.47 \pm 3.15 \text{ W}\cdot\text{m}^{-2}$ (neon Supra'Lux Actizoo 30 W, France). After 35 days, plant clones were acclimatized during 15 days in a new medium, whose chemical composition was identical to that of the Vienne River (Delmail *et al.*, 2011a).

2.2 Plant exposure to Cu or Cd

Explants from acclimatization boxes were transferred into new culture boxes (SteriVent High Model 80 x 110 x 100 mm, KALYS S.A., France) containing 300 mL of fresh oligotrophic medium (10 explants per box; Delmail *et al.*, 2011a). $\text{CuSO}_4 \cdot 5 \text{H}_2\text{O}$ or $\text{CdCl}_2 \cdot 2.5 \text{H}_2\text{O}$ (VWR, Pennsylvania, USA) was added aseptically to the medium in order to obtain an initial concentration ranging from 0.02 to 0.4 μM CuSO_4 and from 1 to 22 nM CdCl_2 (see also Decou *et al.*, 2019). These concentration intervals are close to those measured in the aquatic environment of the Limousin Region. This experiment was conducted over a 27-day period, and biological measurements were recorded every 2 days. Light intensity, photoperiod and temperature all remained the same as those in the micropropagation process. The control (T0) corresponded to the same 14-day *in vitro* acclimatized clones not supplemented by CuSO_4 or CdCl_2 .

2.3 Protein extraction and quantification

The protein extraction protocol was based on the work by Srivastava *et al.* (2006). For each sampling date, 500 milligrams of three independent clones were ground together at 4°C in a

800- μ L buffer containing 50 mM Tris-HCl (pH 7.0), 3.75% polyvinyl pyrrolidone (w/v), 0.1 mM ethylenediaminetetraacetic acid (EDTA) and 1 mM phenylmethylsulfonyl fluoride (Sigma-Aldrich, Missouri, USA). Extracts were centrifuged at 10,000 g for 10 min at 4°C (3-18K centrifuge, Sigma, Germany). The Bradford assay (Bradford, 1976) was applied to measure total protein contents. Fifty μ L of protein extract were added in a cuvette containing 1.5 mL of Bradford Reagent (Sigma-Aldrich, Missouri, USA) and incubated for 15 min at room temperature. The absorbance of the protein-dye complex was read with a spectrophotometer at 595 nm (Helios Beta Thermo Spectronic, Thermo Electron Corporation, USA). The protein concentrations were determined by comparison to the standard curve prepared using the protein standard, i.e. bovine serum albumin (BSA; Sigma-Aldrich, Missouri, USA).

2.4 Watermilfoil enzyme activities

2.4.1 Ascorbate peroxidase

APX activity (EC 1.11.1.11) took place following introduction of a new method based on modifications to Nakano and Asada's method (1981). To measure the rate of ascorbate oxidation into the monodehydroascorbate radical in the presence of H₂O₂, a 3-mL reaction mixture was prepared, containing (in order of addition): 40 mM phosphate buffer (pH 7.8), 0.1 mM EDTA, 0.5 mM sodium ascorbate, 0.1 mM H₂O₂ (Sigma-Aldrich, Missouri, USA), and 0.67% protein extract (v/v). A decrease in the ascorbate absorbance of three technical replicates ensued for 5 min at 266 nm (Helios Beta Thermo Spectronic, Thermo Electron Corporation, USA).

2.4.2 Catalase activity

CAT activity (EC 1.11.1.6) was measured by means of a new improved method based on modifications of the most widespread protocols (Aebi, 1974; Clairbone, 1985). The underlying principle is to measure the H₂O₂ oxidation initiated by CAT. Spectrophotometric measurements were derived from a 3-mL reaction mixture, containing (in order of addition): 50 mM potassium phosphate buffer (pH 7.0), 20 mM H₂O₂ (Sigma-Aldrich, Missouri, USA), and 0.33% protein extract (v/v). A decrease in the H₂O₂ absorbance of three technical replicates ensued for 30 s at 234 nm (Helios Beta Thermo Spectronic, Thermo Electron Corporation, USA).

2.4.3 Glutathione peroxidase

GSH-Px activity (EC 1.11.1.9) was assayed according to a new method inspired from the protocol developed by Jeon *et al.* (2002), which allows measuring the ability of GSH-Px to convert hydroxy and peroxy radicals into water while oxidizing GSH. The oxidized glutathione is then reduced by GR in the presence of NADPH. In this manner, the NADPH oxidation rate is proportional to GSH-Px activity and measured spectrophotometrically as a drop in absorbance at 340nm. The 3-mL reaction mixture was composed of: 50 mM phosphate buffer (pH 7.0), 0.1 mM EDTA, 0.1 mM NADPH, 0.1 mM GSH, 0.1 UI GR, 0.67% protein extract (v/v), and 0.1 mM H₂O₂ (Sigma-Aldrich, Missouri, USA) supplemented with 0.1 mM FeSO₄·7H₂O to produce •OH and HO₂• through the Fenton reaction. The decrease in absorbance of three technical replicates ensued for 10 min (Helios Beta Thermo Spectronic, Thermo Electron Corporation, USA).

2.4.4 Superoxide dismutase

SOD activity (EC 1.15.1.1) was analyzed according to a new method stemming from the protocol by Beauchamp and Fridovich (1971), which enables measuring the ability of SOD to

inhibit the reduction of nitro blue tetrazolium (NBT) into formazan dye in the presence of photochemically produced $O_2^{\bullet-}$. The tubes containing the (3-mL) reaction mixture were composed of: 40 mM phosphate buffer (pH 7.8), 13 mM methionine, 0.1 mM EDTA, 75 μ M NBT (Sigma-Aldrich, Missouri, USA), 20 μ M riboflavin (Duchefa, The Netherlands), and 0.17% protein extract (v/v). All test tubes were shaken and placed 30 cm below the light source ($7.47 \pm 3.15 \text{ W.m}^{-2}$, neon Supra'Lux Actizoo 30W, France) for 8 min. The absorbance of three technical replicates was measured at 560 nm (Helios Beta Thermo Spectronic, Thermo Electron Corporation, USA).

2.5 Trace metals in plants

The metals found in samples were measured using ICP-MS (SCIEX-ELAN 6100 DRC, PerkinElmer, Massachusetts, USA). For plant mineralization, three independently gathered watermilfoil clones were carefully rinsed with distilled water and blotted dry; also, 500 mg fresh weight were digested in 2.5 mL HNO_3 69% (Fisher chemical, Thermo Fisher Scientific, USA) at 60°C for 48 h. Five hundred microliters of the solution were diluted in 2 mL of aqueous solution (4.5‰ n-butanol, 0.1 $g.L^{-1}$ ammonia, 0.1 $g.L^{-1}$ EDTA, 1‰ germanium as the internal standard) and then introduced into the nebulizer. Five-point reference scales were applied according to the same protocol as before (from 0.1 to 10 $\mu g.L^{-1}$ Cd and 0.5 to 50 $\mu g.L^{-1}$ Cu). For each biological sample, three technical replicates were performed. The limits of quantification (LQ) were: 0.1 $\mu g.L^{-1}$ for Cd, and 0.5 $\mu g.L^{-1}$ for Cu. The Plasma Power, Plasma Gas Flow and Auxiliary Gas Flow equaled 1,350 W, 15 $L.min^{-1}$ and 1.175 $L.min^{-1}$, respectively.

2.6 Statistical analyses

Physiological measurements were carried out in triplicate. The software R 2.11.0 (R Foundation, Austria) was run for this statistical analysis. The normality of the measurement data matrix was tested with the Multivariate Shapiro-Francia test (Delmail *et al.*, 2011c); its result indicated that APX and SOD activities followed a normal distribution ($P > 0.05$), as did the CAT and GSH-Px activities ($P > 0.05$). Hence, a parametric hierarchical cluster analysis (HCA) using Ward's method and a non-parametric HCA were both applied on APX/SOD data and CAT/GSH-Px data, respectively, to assess and determine the enzymatic behavior of *M. alterniflorum* when exposed to different concentrations of Cd and Cu.

Journal Pre-proof

3. Results

Cadmium and copper accumulation in *M. alterniflorum* were already published in Decou *et al.* (2019). These results showed a fast phyto-absorption of metals from the first days after exposure followed by slower accumulation until the end of the experiment (however, Cu was more quickly phyto-accumulated than Cd).

The activity profiles obtained for each antioxidant enzyme are presented in the supplementary figures (Figs. S1, S2, S3 and S4). For the sake of clarity, the overall results of Figures S1-4 have been proposed in a single figure (Fig. 1), which more easily shows the oxidative-stress periods. In this figure, the entire activity profiles obtained at all Cd or Cu concentrations are represented as sixth-order polynomial trendlines, and the response intensity proportions between Cu and Cd profiles have been retained for each considered enzyme. Each trendline was automatically generated using the 2016 Microsoft Excel spreadsheet software.

3.1 Watermilfoil ascorbate-peroxidase activities

The APX activities of *M. alterniflorum* did not appear to be highly homogeneous for all Cd treatments performed over 27 days ($p = 0.315$; Figs. 1 and S1). For this reason, HCA were performed to provide clustering analyses, yielding trends difficult to identify from raw data. As such, the only clade observed for APX was formed by 2 and 9 nM CdCl₂ activity profiles (clade 1, Fig. 2a), yet it showed very weak homogeneity ($p = 0.106$). On the other hand, the two other activity profiles at 15 and 22 nM CdCl₂ displayed greater homogeneity between each other over the entire analysis interval ($p = 0.488$) and with 1 nM CdCl₂ as well ($p = 0.554$ and $p = 0.614$, respectively; see also Supplementary text, Part 1a). This observation is clearly confirmed by the corresponding polynomial trendlines, which show a major response to an oxidative stress over the first 11 days for both 15 and 22 nM CdCl₂ (Fig. 1). In addition, this response appears to be correlated with Cd concentration. In contrast, a shift in the APX

response is observed for weaker Cd concentrations since the most intense activity has been obtained from Day 13 to Day 23 (Figs. 1 and S1).

According to the Cu exposure over 27 days, watermilfoil APX activities were relatively homogeneous ($p = 0.550$). As opposed to Cd treatments, HCA revealed three clades (Fig. 2b), with their Euclidean positions being explained by similarities between activity profiles (Supplementary text, Part 2a). Although three peaks were obtained from 0 to 15 days for all Cu treatments (Fig. S1), the graphical depiction of APX activities by polynomial trendlines provided a single overall peak for 0.04, 0.1 and 0.4 μM CuSO_4 , while two peaks were observed for 0.02 and 0.2 μM CuSO_4 (Fig. 1). This single overall peak was pronounced for the higher Cu concentration at 0.4 μM CuSO_4 ; however, the intensity of the APX response did not seem to be correlated with Cu concentration or at least only slightly correlated, albeit with a rather disorganized time response (Figs. 1 and S1).

3.2 Watermilfoil catalase activities

Over the entire analysis, the Cd range remained relatively heterogeneous ($p = 0.037$), thus explaining the presence of just one clade (Fig. 3a; $p = 0.364$ between 2 and 9 nM CdCl_2). Moreover, despite the difference in the number of peaks for clade 1, three peaks were very similar in terms of duration between each activity profile (Fig. S2 and Supplementary text, Part 1b). This finding was clearly observed as well by the corresponding polynomial trendlines (Fig. 1). In addition, the features of the 1 nM CdCl_2 polynomial trendline were similar to this general profile at weak Cd concentrations (Fig. 1), which was in close agreement with the Euclidean position (Fig. 3a). However, in a general way for low Cd concentrations, an initial CAT activity response was detected during the second week of analysis and then followed by a higher response during the last week. When the Cd

concentration increased, these two activity “waves” appeared earlier and with greater intensity (Fig. 1).

As opposed to Cd exposure, the agglomerative hierarchical clustering analyses of watermilfoil CAT activities during Cu treatments indicated two clades, which were highly discriminated ($p = 0.007$ between 0.04 and 0.4 μM CuSO_4 , $p = 0.047$ between 0.1 and 0.04 μM CuSO_4 , and $p = 0.025$ between 0.1 and 0.4 μM CuSO_4 , Fig 3b). This heterogeneity between CAT profiles was clear, and the association of a number of specific peaks could be explained in distinct clades (Fig. S2 and Supplementary text, Part 2b). Similarly, polynomial trendlines clearly underscored the differences between the CAT activity profiles and highlighted their Euclidean distribution (Fig. 1). Nevertheless, an analogous increase in activity was noted for all profiles during the final 4-6 days of Cu exposure (Fig. 1).

3.3 Watermilfoil glutathione-peroxidase activities

The GSH-Px range was moderately homogeneous during 27 days of watermilfoil Cd exposure ($p = 0.569$, Figs. 1 and S3). Three clades were observed from the HCA analysis (Fig. 4a), with clade 1 presenting the greatest homogeneity across all groups ($p = 0.812$ between 1 and 2 nM CdCl_2). The 22 nM CdCl_2 profile composing clade 2 was placed as an *outgroup* of clade 1. The homogeneity levels measured were: $p = 0.208$ with 1 nM CdCl_2 , and $p = 0.209$ with 2 nM CdCl_2 . The Euclidean position assessment of each profile was quite difficult to analyze, yet some trends could be drawn to explain the HCA (Supplementary text, Part 1c).

Nevertheless, two very weak responses to oxidative stress seemed to be apparent regardless of the Cd concentration used: one during the first week, the other during the period from Day 11 to Day 23 (Fig. 1). Interestingly, a sharp increase in intensity was observed during the final

days of the assay for concentrations at 9, 15 and 22 nM CdCl₂ (corresponding mainly to clade 3, Fig. 4a).

As for the Cd treatments, the HCA of GSH-Px during Cu exposure was characterized by three clades (Fig. 4b). The homogeneity of all activities covering the entire period of analysis was also notably low ($p = 0.342$, Figs. 1 and S3) despite the presence of common peaks at nearly the same date for all Cu treatments (Supplementary text, Part 2c). The distribution of activity profiles according to HCA analysis (Fig. 4b) was therefore due to differences over shorter time intervals. A fast response was in fact measured during the first 5 days for all Cu concentrations employed (except 0.04 μM CuSO₄, which displayed a peak at 7 days, Fig. 1). Next, a second increase was detected between 9 and 21 days, once again depending on the Cu concentration used. Lastly, a strong increase in GSH-Px activity was recorded for higher Cu concentrations over the last 4 days (to a lesser extent as well for 0.02 μM CuSO₄), which was in agreement with the clade distribution (Fig. 4b).

3.4 Watermilfoil superoxide-dismutase activities

Similarly to the HCA obtained from GSH-Px profiles during Cd treatments, Cd concentrations at 9 and 15 nM CdCl₂ as well as at 1 and 2 nM CdCl₂ constituted two distinct clades for SOD activities (Fig. 5a). The low homogeneity of clade 2 (1 and 2 nM CdCl₂) with both clade 1 and 22 nM CdCl₂ profiles ($0.148 < p < 0.433$) explained its isolated Euclidean position. However, SOD activity profiles (Fig. 1) showed similar polynomial trendlines for 2 and 22 nM CdCl₂ while 9 and 15 nM CdCl₂ seemed to differ (clade 2). The sharp increase in SOD activity during the final four days could probably manage the clade distribution (Fig. 5a), although other peak analogies could explain this as well (Supplementary text, Part 1d).

Nevertheless, an initial and weak SOD response to oxidative stress was observed during the first five days for all Cd treatments applied (Figs. 1 and S4).

A clear heterogeneity ($p = 0.058$) was derived for all SOD activity profiles during Cu exposure, which serves to simplify the understanding of clade composition (Fig. 5b). The Euclidean positions of 0.04 and 0.1 μM CuSO_4 profiles assembled in clade 1 ($p = 0.933$) were indeed justified by the presence of identical peaks at the same intervals (Supplementary text, Part 2d). This association in clade 1 however was not as obvious to observe with polynomial trendlines (Fig. 1). In contrast, the Euclidean positions of clade 2 and the 0.2 μM CuSO_4 profile were more easily justified given that the trendlines expressed similarities throughout the experiment (Fig. 1).

4. Discussion

4.1 Impact of Cd on the APX, CAT, GSH-Px and SOD activities

Cadmium is a toxic and non-essential microelement that does not participate in cell metabolism. The physicochemical properties of Cd^{2+} ions are similar to those of Ca^{2+} , in allowing Cd^{2+} to pass through the biological membranes and accumulate in tissues (Faller *et al.*, 2005; Drażkiewicz and Baszyński, 2008). In plants, Cd toxicity is generally due to its association with sulfhydryl groups (-SH) of proteins, which induces enzyme inhibition, a modification of the cell redox control and ROS overproduction (Romero-Puertas *et al.*, 2004; Wawrzyński *et al.*, 2006). Since the release of these compounds in cell compartments produces an oxidative stress - as already observed through different biological parameters in *M. alterniflorum* (Delmail *et al.*, 2011a,b) or in *Myriophyllum quitense* (Nimptsch *et al.*, 2005) - this last one could be followed through four detoxifying enzymes (APX, CAT, GSH-Px and SOD) correlated primarily with H_2O_2 or $\text{O}_2^{\bullet-}$ scavenging.

As observed in Decou *et al.* (2019), Cd was quickly phyto-accumulated in *M. alterniflorum* with an apparent stabilization of the concentration from 17 to 27 days. Therefore, we concluded that the fast Cd bioaccumulation in plants complicated the definition of biomarker-response origins during the 1-27-day period. Nevertheless, early biomarker responses due to this quick metal element accumulation could be expected. Here, an initial oxidative stress was indeed detected during the first ten days of watermilfoil Cd exposure for APX and CAT. Moreover, the response intensity of both enzymes appeared to be correlated with the Cd concentration (already highlighted for vitamin E and malondialdehyde biomarkers in *M. alterniflorum*; Decou *et al.*, 2019), which is in agreement with the Euclidean positions of their respective HCA. This correlation was also denoted in the aquatic plant *Ceratophyllum demersum* (Kováčik *et al.*, 2017). Moreover, the CAT response speed was greater at stronger Cd concentrations, thus indicating the importance of the redox disturbance mostly at higher

concentrations. However, the fact that the response to oxidative stress appears later at weaker Cd concentrations, suggests that a strong metal stress has priority for rapid detoxification, whereas a weak metal stress could be managed subsequently in order to allocate more energy to other types of toxic compound detoxification. In addition, this handling delay could be due to a low chloroplastic H₂O₂ production, which needs to reach a threshold concentration for the APX synthesis due in general to its positive correlation with the chloroplastic H₂O₂ concentration (Hu *et al.*, 2008; Mittler, 2002). H₂O₂ in *Ceratophyllum demersum* was indeed poorly detected at low Cd concentration exposure (10 μM) but highly observable by microscopy during a 100 μM Cd treatment of the plants (Kováčik *et al.*, 2017). Interestingly, the CAT activity response differed slightly from that of APX, as a second oxidative burst was detected throughout the analysis period (appearing earlier for higher concentrations), thus suggesting the need to remove more H₂O₂ for cell rescue. However, this second burst could seem surprising given the almost stable Cd phyto-accumulation in watermilfoil from the 17th day. This result suggested a *de novo* H₂O₂ production maybe as a consequence of the O₂•⁻ dismutation by SOD enzymes.

All these data support the critical role of CAT in H₂O₂ scavenging, as observed in *Arabidopsis* and tobacco (Queval *et al.*, 2007; Su *et al.*, 2018). Peroxisomes are indeed a significant source of H₂O₂ in plant cells and the main subcellular localization of CAT. Therefore, this enzyme localization appears to be paramount during the H₂O₂ overproduction generated by metal stress. Furthermore, the strong CAT activity during high Cd exposure could reflect a major H₂O₂ diffusion to the peroxisomes for unblocking this ROS accumulation in cytosol or in more sensitive organelles, like chloroplasts and mitochondria. Moreover, H₂O₂ diffusion from chloroplasts, probably through aquaporins, was already demonstrated in *Spinacia oleracea* L. and could trigger signaling processes in the cytoplasm or nucleus in order to change the expression level of responsive genes (Mubarakshina *et al.*,

2010). However, it is important to note that H_2O_2 accumulation could also be due to ROS directly produced in peroxisome. Indeed, this organelle contains H_2O_2 generating enzymes that can be upregulated during metal stress (Romero-Puertas *et al.*, 2019).

In contrast, the polynomial trendlines of GSH-Px and SOD (Fig. 1) were very similar. This finding was not surprising given that the clade composition is nearly identical (Figs. 4a and 5a). An oxidative stress probably appeared between 0 and 5-7 days, though at a very low intensity compared to the other two detoxifying enzymes (APX and CAT). Therefore, $\text{O}_2^{\bullet-}$ would be rapidly converted spontaneously to H_2O_2 by dismutation even in the absence of SOD (Romero-Puertas *et al.*, 2019; Zhuang *et al.*, 2019). Since reduced GSH is used as a substrate for both GSH-Px and phytochelatin synthase (PCS), the limited GSH-Px activity could correspond to an allocation of GSH priority to PCS. GSH is actually being more heavily solicited for PC production (Rausch *et al.*, 2007), as observed in *A. thaliana* (Gielen *et al.*, 2017). GSH might also be used for the chloroplastic ascorbate reduction via the glutathione dehydrogenase (Møller, 2001). However, even if the activity levels of GSH-Px and SOD in response to oxidative stresses were not so pronounced, some interval shifting did appear, depending on Cd concentration (more specifically, the higher the concentration, the later the response). Surprisingly, a sudden oxidative stress was primarily identified at higher toxic metal concentrations during the final day of the assay. Consequently, the hypothesis of a strong release or accumulation of $\text{O}_2^{\bullet-}$ can be forwarded since this molecule is being used like a substrate by the SOD enzymes, especially in chloroplasts and mitochondria. The photosystem I and II, complex I, ubiquinone and complex III of the electron transport chain constitute the major sites for generating $\text{O}_2^{\bullet-}$ (Gill and Tuteja, 2010). Indeed, as suggested by Zhuang *et al.* (2019) during nitrogen stresses in *Hydrilla verticillata*, alterations in the photosynthetic electron transfer chain could lead to $\text{O}_2^{\bullet-}$ production. Consequently, the H_2O_2

overproduction generated by SOD, following the chloroplastic $O_2\bullet^-$ release, has probably led to the *de novo* activity of GSH-Px and, to a lesser extent, APX (Fig. 1).

According to the localization of these four enzymes, their activity profiles point to an oxidative stress management mainly during the first three weeks in peroxisomes and chloroplasts, as demonstrated by CAT and APX, respectively (more activity was detected in the first ten days). Later, during the final week of Cd exposure, this oxidative stress was still occurring in chloroplasts (weaker), but also in mitochondria, cytosol and all cell compartments, as indicated by SOD and GSH-Px activity. Generally speaking, the significant ROS scavenging in chloroplasts is mainly due to the extensive ROS production in this cell compartment, as well as to its photoactive nature (Gill and Tuteja, 2010). A previous study on *M. alterniflorum* also demonstrated the negative effect of Cd, especially on chloroplasts and their photosynthetic pigment content (Delmail *et al.*, 2011b). It is likely therefore that plants favor the chloroplast protection in order to preserve their photosynthetic capacities. Although SOD and GSH-Px activities displayed a weak response during the first week after Cd treatment, a fast response (from Day 0 to Day 3) could still be detected. This finding suggests the quick removal of another ROS ($\bullet OH$) along with H_2O_2 in preventing against their excessive cell accumulation. This result however is at odds with the acknowledged role of SOD since this enzyme is considered to represent the first line of antioxidant defense against a potent ROS like $O_2\bullet^-$ (Gill *et al.*, 2016). Consequently, the chronology of the defense strategy involving different organelles cannot be clarified with certainty given the large number of enzyme isoforms and their subcellular localization specificity (i.e. proposed SOD subcellular localizations in mitochondria (MSD1), chloroplasts (CSD2, FSD2 and 3), peroxisome (CSD3) and cytosol (CSD1); Pilon *et al.*, 2011). Moreover, differential compensatory mechanisms for Cd detoxification were reported in aquatic plants (*Pistia stratiotes* and *Eichhornia crassipes*, Toppi *et al.*, 2007; *Taxiphyllum barbieri* (moss) and

Ceratophyllum demersum (macrophyte), Kováčik *et al.*, 2017). These make the strategies of plant antioxidant defense more difficult to understand and to highlight. Finally, in spite of the acclimatization period, results from *in vitro* cultures might induce biochemical changes that have not been observed in field plants, although from another perspective various uncontrolled environmental factors from *in situ* experiments also affect the biochemical responses.

4.2 Impact of Cu on the APX, CAT, GSH-Px and SOD activities

Copper is involved in many redox processes under Cu^{2+} and Cu^+ forms, and moreover is considered as a key micronutrient in cell metabolism. For example, copper participates in photosynthesis, mitochondrial respiration, oxidative stress and hormonal signalization via ROS production, yet it is also a structural element for proteins (Cu/Zn-SOD, cytochrome C oxidase, plastocyanins, laccases, etc.; Pilon *et al.*, 2006). Cu excess or deficiency leads to major disruptions in plant development and growth since the photosynthetic machinery is principally affected (Costa *et al.*, 2018; Krayem *et al.*, 2018). During Cu excess, a strong redox effect can also be generated. Consequently, ROS are produced and induce severe nuclear, lipid and protein damages (Yruela, 2005).

In vitro Cu phyto-accumulation was extremely rapid (most of the metal accumulated one day after exposure; Decou *et al.*, 2019). Consequently, the Cu concentration in the medium drastically changed contrary to *in situ* conditions where aquatic plants are permanently exposed to a quite stable metal concentration in surface waters (apart from pollution peaks). Therefore, this bioaccumulation pattern makes more difficult the biomarker response profile analysis. Nevertheless, as for Cd exposure, APX, CAT, GSH-Px and SOD activities were analyzed, and their intensities yielded information on the oxidative stresses appearing in watermilfoil plants. For example, the raw results from APX activities (Fig. S1) revealed

numerous peaks during the first 15 days at all Cu concentration levels tested. The merged results (polynomial trendlines, Fig. 1) however showed a single primary increase in APX activity during this period, corresponding to an overall oxidative stress attributable to H₂O₂. It is worth noting that the response intensity does not seem to be positively correlated with Cu concentration. In contrast, CAT activities revealed specific responses that were quite different from those obtained for Cd exposure. The two clades and activity profiles (Figs. 3 and 1) already indicated the absence of any correlation between CAT activity intensity or time response and Cu concentration. The analysis of CAT activities was therefore rather complicated yet still suggested that antioxidant system damage occurred beyond 0.1 µM CuSO₄ given the observed decrease in CAT activity at 0.2 and 0.4 µM CuSO₄. Interestingly, the competition of Cu²⁺ with Fe²⁺ could induce deficiency of the latter during plant absorption (Bernal *et al.*, 2007). CAT does in fact require Fe²⁺ in its heme structure, and this enzyme is already known to be negatively affected by oxidative stress in a state of Fe²⁺ deficiency (Tewari *et al.*, 2005). As a result, Fe²⁺ starvation at higher Cu concentrations probably causes the CAT activity disruption. Moreover, Fe²⁺ deficiency in plant cells significantly reduces ROS production, further disturbing the Fenton and Haber-Weiss reactions responsible for generating •OH (Tewari *et al.*, 2005; Ranieri *et al.*, 2001; Drazkiewicz *et al.*, 2004). A high Cu exposure could thus limit the oxidative stress, and a threshold impossible to exceed could be reached over 0.1 µM CuSO₄ in the case of antioxidant enzymes. Interestingly, these limitations were also observed for three other biomarkers such as glucose-6-phosphate dehydrogenase, malondialdehyde and α-tocopherol (Decou *et al.*, 2019). Since photosynthetic pigments lie on the frontline of ROS during metal stress, this hypothesis could be strengthened by the absence of any Cu impact on *M. alterniflorum* photosynthetic pathways, as described by Delmail *et al.* (2011a), although these authors did not precisely analyze the photosynthetic process in itself.

As regards SOD and GSH-Px activities, similar polynomial trendlines were observed for both enzymes (Fig. 1). A fast but weak response was measured over the first 5 days, followed by a second increase during the next two weeks. Afterwards, a large stress due to $O_2\cdot^-$, $\cdot OH$ and H_2O_2 , probably in both chloroplasts and mitochondria, could be clearly observed during the last week for high Cu concentrations. Indeed, the strong impact of this pollutant on these organelles were several times reported, for example, in *Ceratophyllum demersum* (Cu toxicity damages, before anything else, the reaction centre of the photosystem II; Thomas *et al.*, 2013, 2016) or in *Pistia stratiotes* (exposure to elevated concentration of Cu produced ultrastructural changes - shrinkage and distortion - of chloroplast and mitochondria; Upadhyay and Panda, 2009). This increase also occurred during Cd treatments, albeit to a lesser extent. All these results indicating the absence of strong oxidative stress during the first three weeks suggest the presence of other detoxification systems, like PC, GSH, ascorbic acid or α -tocopherols, which were favored in response to watermilfoil Cu treatments. Moreover, PC, which chelate trace-metal ions in plants (Anjum *et al.*, 2015), could become overexpressed and thereby limit the presence of intracellular Cu^{2+} . Besides the potential Fe^{2+} deficiency, the absence of divalent ions would reduce ROS production and, consequently, shed light on the limited antioxidant response observed at high Cu concentrations. These results might also explain why the highest Cu concentrations were found with $0.02 \mu M$ $CuSO_4$ in the same clades (Figs. 4b and 5b). Previous results already demonstrated the decline of antioxidant enzyme activities (mostly APX and guaiacol peroxidase) beyond a moderate Cu exposure in *Hydrilla verticillata* (Srivastava *et al.*, 2006). Lastly, in order to protect the young part of plants, the presence of an ultimate oxidative stress detected at the end of the experiment could correspond to the ROS produced by metal accumulation in the old senescent leaves (Delmail *et al.*, 2011a).

4.3 Assessment of Cu or Cd impact on antioxidant enzyme activities

Altogether, biochemical data obtained from *M. alterniflorum* Cu or Cd exposure seemed to indicate a specific strategy of ROS regulation in this aquatic plant since the scientific literature mostly demonstrates the ROS management by SOD during the first days of metal treatment. Here, APX and CAT appeared as the frontline enzymes (from the four tested) for ROS removing at highest Cu or Cd concentrations. With regard to the putative subcellular localizations of these enzymes, production of H₂O₂ strongly occurred in chloroplasts (for high Cu toxicity) or in peroxisomes (for high Cd toxicity). This difference could probably be explained by the characteristic “essential” or “not essential” for plants of these metal compounds. Indeed, *M. alterniflorum* would limit the Cd impact on photosynthetic and respiratory machineries by promptly relocated H₂O₂ in peroxisome. At the contrary, as Cu is involved in chloroplastic functions and plays a vital role in maintaining normal metabolism, its toxicity on photosynthesis (i.e pigments and protein components of photosynthetic membranes used as targets, disturbances in the uptake of other essential elements; Pätsikkä *et al.*, 2002) constrains the plants to foil the imbalance in chloroplasts as a matter of priority, especially as CAT activity is probably negatively affected by a Fe²⁺ deficiency.

As an excess of ROS is dangerous for the cell homeostasis and survival, we could show here and in previous studies, the importance and complementarity of both watermilfoil enzymatic and non-enzymatic antioxidant systems for cell recovery during Cu or Cd stresses. However, as in Decou *et al.* (2019), long-term *in situ* evaluation of antioxidant enzymes from *M. alterniflorum* associated to physico-chemical analyses should be done for perceiving this aquatic plant as a robust bioindicator of water contamination by metal compounds.

5. CONCLUSION

The results presented here have clearly shown the complexity of the ROS scavenging biochemical mechanisms, as demonstrated by the enzyme activity featuring specific or unspecific profiles depending on both metal concentration and time exposure. Admittedly, it sometimes seems difficult to draw a conclusion with absolute certainty on the level of enzyme involvement in the detoxification process, given the multitude of contributing actors (organites, enzymes, scavengers, etc.) and their own sensitivity to toxic compounds. Nevertheless, the HCA and activity profiles of the four analyzed enzymes have yielded preliminary information regarding both cellular oxidative patterns and *M. alterniflorum* strategies for metal stress management. In general, it would appear that the cells follow a detoxifying program corresponding to a series of "enzyme kicks", which initially favors the removal of more toxic compounds and, preferentially, the protection of chloroplasts, as observed in the APX activity for both metal stresses. However, the four enzyme activities monitored in this study cannot on their own explain the high oxidative stress phase management as other scavenging pathways and developmental changes occur. In addition, beyond the ROS elimination processes used by plant cells, the chemical nature of the toxic compound is also of paramount importance by virtue of limiting the oxidative stress in spite of its relative toxicity. Competition with other essential plant ions has been assumed here between Cu^{2+} and probably Fe^{2+} . Therefore, given that enzyme activity profiles of watermilfoil seem to reflect the oxidative stresses generated by metal compounds, the monitoring of these biological parameters should be considered during ecological surveys conducted in streams. Associated to physico-chemical parameters, to chemical passive monitoring and to complementary watermilfoil non-enzymatic biomarkers, such studies would allow to better understand the plant defense systems and to develop a methodology for water-quality biomonitoring. Moreover, metal-specific molecular biomarkers like PC, PCS

activity and its genic expression should be considered in further studies. All of these elements will allow to definitively adopt, or not, this plant as a paramount bioindicator of surface waters. However, even though *in situ* data represent an evident transition for biomonitoring research, the multitude of parameters influencing the biological development of aquatic plants represent a tall order in terms of technical abilities and data integration. Organic pollutants are for example a major problematic given their number and our inability, currently, to detect all of them.

Conflicts of Interest

The authors have declared no conflicts of interest.

Compliance with Ethics Requirements

This article does not entail any studies using human or animal subjects.

ACKNOWLEDGMENTS

This financing for this research effort had three sources: the European Union, through the FEDER-Plan Loire project "MACROPOD 2 2016EX-000856", for R. Decou's post-doctoral fellowship; the Limousin Regional Council for D. Delmail's PhD thesis; and the PEIRENE EA7500 Laboratory (formerly GRESE EA 4330).

REFERENCES

- Aebi, H., 1974. Catalase. In Bergmeyer, H. U., ed. *Methods of enzymatic analysis*. New York and London: Academic Press. 673-677.
- Alscher, R.G., Erturk, N., Heath, L.S., 2002. Role of superoxide dismutases (SODs) in controlling oxidative stress in plants. *J. Exp. Bot.* 53(372), 1331-1341. <https://doi.org/10.1093/jexbot/53.372.1331>
- Anjum, N.A., Hasanuzzaman, M., Hossain, M.A., Thangavel, P., Roychoudhury, A., Gill, S.S., Merlos Rodrigo, M.A., Adam, V., Fujita, M., Kizek, R., Duarte, A.C., Pereira, E., Ahmad, I., 2015. Jaks of metal/metalloid chelation trade in plants—an overview. *Front. Plant Sci.* 6(192), 1-17. <https://doi.org/10.3389/fpls.2015.00192>
- Anjum, N.A., Sharma, P., Gill, S.S., Hasanuzzaman, M., Khan, E.A., Kachhap, K., Mohamed, A.A., Thangavel, P., Devi, G.D., Vasudhevan, P., Sofu, A., Khan, N.A., Misra, A.N., Lukatkin, A.S., Singh, H.P., Pereira, E., Tuteja, N., 2016. Catalase and ascorbate peroxidase-representative H₂O₂-detoxifying heme enzymes in plants. *Environ. Sci. Pollut. Res.* 23, 19002-19029. <https://doi.org/10.1007/s11356-016-7309-6>
- Beauchamp, C.O., Fridovich, I., 1971. Superoxide dismutase: improved assays and an assay applicable to acrylamide gels. *Anal. Biochem.* 44, 276-287. [https://doi.org/10.1016/0003-2697\(71\)90370-8](https://doi.org/10.1016/0003-2697(71)90370-8)
- Bernal, M., Cases, R., Picorel, R., Yruela, I., 2007. Foliar and root Cu supply affect differently Fe- and Zn-uptake and photosynthetic activity in soybean plants. *Environ. Exp. Bot.* 60, 145-150. <https://doi.org/10.1016/j.envexpbot.2006.09.005>
- Bolwell, G.P., Wojtaszek, P., 1997. Mechanisms for the generation of reactive oxygen species in plant defense – a broad perspective. *Physiol. Mol. Plant Pathol.* 51(6), 347-366. <https://doi.org/10.1006/pmpp.1997.0129>

Bradford, M.M., 1976. A rapid and sensitive method for the quantitation of microgram quantities of protein utilizing the principle of protein-dye binding. *Anal. Biochem.* 72, 248-254. [https://doi.org/10.1016/0003-2697\(76\)90527-3](https://doi.org/10.1016/0003-2697(76)90527-3)

Claiborne, A., 1985. Catalase activity. In: Greenwald R.A., ed. CRC. *Handbook of methods for oxygen radical research*. Boca Raton, FL, USA: CRC Press. 283-284.

Costa, M.B., Tavares, F.V., Martinez, C.B. Colares, I.G., Martins, C de M.G., 2018. Accumulation and effects of copper on aquatic macrophytes *Potamogeton pectinatus* L.: Potential application to environmental monitoring and phytoremediation. *Ecotox. Environ. Safety.* 155, 117-124. <https://doi.org/10.1016/j.ecoenv.2018.01.062>

Das, K., Roychoudhury, A., 2014. Reactive oxygen species (ROS) and response of antioxidants as ROS-scavengers during environmental stress in plants. *Front. Environ. Sci.* 2(53), 1-13. <https://doi.org/10.3389/fenvs.2014.00053>

Decou, R., Laloi, G., Zouari, M., Labrousse, P, Delmail, D., 2018. Evaluation of the relevance of *Myriophyllum alterniflorum* (Haloragaceae) cadmium-sensitive biomarkers for ecotoxicological surveys. *Bull. Environ. Contam. Toxicol.* 101,458-466. <https://doi.org/10.1007/s00128-018-2433-2>

Decou, R., Bigot, S., Hourdin, P., Delmail, D., Labrousse, P., 2019. Comparative *in vitro/in situ* approaches to three biomarker responses of *Myriophyllum alterniflorum* exposed to metal stress. *Chemosphere*, 222, 29-37. <https://doi.org/10.1016/j.chemosphere.2019.01.105>

Delmail, D., Labrousse, P., Hourdin, P., Larcher, L., Moesch, C., Botineau, M., 2011a. Differential responses of *Myriophyllum alterniflorum* DC (Haloragaceae) organs to copper: physiological and developmental approaches. *Hydrobiologia.* 664, 95-105. <https://doi.org/10.1007/s10750-010-0589-9>

Delmail, D., Labrousse, P., Hourdin, P., Larcher, L., Moesch, C., Botineau, M., 2011b. Physiological, anatomical and phenotypical effects of a cadmium stress in different-aged

chlorophyllian organs of *Myriophyllum alterniflorum* DC (Haloragaceae). *Environ. Exp. Bot.* 72, 174-181. <https://doi.org/10.1016/j.envexpbot.2011.03.004>

Delmail, D., Labrousse, P., Botineau, M., 2011c. The most powerful multivariate normality test for plant genomics and dynamics data sets. *Ecol. Informatics*. 6, 125-126.

Delmail, D., Labrousse, P., 2012. Plant ageing, a counteracting agent to xenobiotic stress". In *Senescence*, Nagata, T., ed. 89–106. Rijeka: InTech Publishers. IntechOpen, DOI: 10.5772/31944. Available from: <https://www.intechopen.com/books/senescence/plant-ageing-a-counteracting-agent-to-xenobiotic-stress>

Delmail, D., Labrousse, P., Hourdin, P., Larcher, L., Moesch, C., Botineau, M., 2013. Micropropagation of *Myriophyllum alterniflorum* (Haloragaceae) for stream rehabilitation: first *in vitro* culture and reintroduction assays of a heavy-metal hyperaccumulator immersed macrophyte. *Int. J. Phytoremediat.* 15(7), 647-662. <https://doi.org/10.1080/15226514.2012.723068>

Drazkiewicz, M., Skórzynska-Polit, E., Krupa, Z., 2004. Copper induced oxidative stress and antioxidant defense in *Arabidopsis thaliana*. *Biometals*. 17, 379–387. <https://doi.org/10.1023/B:BIOM.0000029417.18154.22>

Drażkiewicz, M., Baszyński, T. 2008. Calcium protection of PS2 complex of *Phaseolus coccineus* from cadmium toxicity: *in vitro* study. *Environ. Exp. Bot.* 64, 8-14. <https://doi.org/10.1016/j.envexpbot.2007.12.010>

Faller, P., Kienzler, K., Krieger-Liszkay, A., 2005. Mechanism of Cd²⁺ toxicity: Cd²⁺ inhibits photoactivation of Photosystem II by competitive binding to the essential Ca²⁺ site. *Biochim. Biophys. Acta*. 1706, 158-164. <https://doi.org/10.1016/j.bbabbio.2004.10.005>

Gao, J., Ren, P., Zhou, Q., Zhang, J., 2019. Comparative studies of the response of sensitive and tolerant submerged macrophytes to high ammonium concentration stress. *Aquat. Toxicol.* 211, 57-65. <https://doi.org/10.1016/j.aquatox.2019.03.020>.

Gielen, H., Vangronsveld, J., Cuypers, A., 2017. Cd- induced Cu deficiency responses in *Arabidopsis thaliana*: are phytochelatins involved? *Plant Cell Environ.* 40, 390–400. doi: 10.1111/pce.12876. <https://doi.org/10.1111/pce.12876>

Gill, S.S., Tuteja, N., 2010. Reactive oxygen species and antioxidant machinery in abiotic stress tolerance in crop plants. *Plant Physiol. Biochem.* 48, 909-930. <https://doi.org/10.1016/j.plaphy.2010.08.016>

Gill, S.S., Anjum, N.A., Gill, R., Yadav, S., Hasanuzzaman, M., Fujita, M., Mishra, P., Sabat, S.C., Tuteja, N., 2015. Superoxide dismutase-mentor of abiotic stress tolerance in crop plants. *Environ. Sci. Pollut. Res.* 22, 10375–10394. <https://doi.org/10.1007/s11356-015-4532-5>

Harguinteguy, C.A., Schreiber, R., Pignata, M.L., 2013. *Myriophyllum aquaticum* as a biomonitor of water heavy metal input related to agricultural activities in the Xanaes River (Córdoba, Argentina). *Ecol. Indic.* 27, 8-16. <https://doi.org/10.1016/j.ecolind.2012.11.018>

Harguinteguy, C.A., Cofré, M.N., Fernández-Cirelli, A., Pignata, M.L., 2016. The macrophytes *Potamogeton pusillus* L. and *Myriophyllum aquaticum* (Vell.) Verdc. as potential bioindicators of a river contaminated by heavy metals. *Microchem. J.* 124, 228-234. <https://doi.org/10.1016/j.microc.2015.08.014>

Harguinteguy, C.A., Gudiño, G.L., Arán, D.S., Pignata, M.L., Fernández-Cirelli, A., 2019. Comparison between two submerged macrophytes as biomonitors of trace elements related to anthropogenic activities in the Ctalamochita River, Argentina. *Bull. Environ. Contam. Toxicol.* 102(1), 105-114. <https://doi.org/10.1007/s00128-018-2499-x>

Hu, W.H., Song, X.S., Shi, K., Xia, X.J., Zhou, Y.H., Yu, J.Q., 2008. Changes in electron transport, superoxide dismutase and ascorbate peroxidase isoenzymes in chloroplasts and mitochondria of cucumber leaves as influenced by chilling. *Photosynthetica.* 46, 581-588. <https://doi.org/10.1007/s11099-008-0098-5>

Jeon, S.M., Bok, S.H., Jang, M.K., Kim, Y.H., Namc, K.T., Jeong, T.S., Park, Y.B., Choi, M.S., 2002. Comparison of antioxidant effects of naringin and probucol in cholesterol-fed rabbits. *Clin. Chim. Acta.* 317, 181-190. [https://doi.org/10.1016/S0009-8981\(01\)00778-1](https://doi.org/10.1016/S0009-8981(01)00778-1)

Kärkönen, A., Kuchitsu, K., 2015. Reactive oxygen species in cell wall metabolism and development in plants. *Phytochem.* 112, 22-32. <https://doi.org/10.1016/j.phytochem.2014.09.016>

Krayem, M., Deluchat, V., Hourdin, P., Fondanèche, P., Lecavelier Des Etangs, F., Kazpard, V., Moesch, C., Labrousse, P., 2018. Combined effect of copper and hydrodynamic conditions on *Myriophyllum alterniflorum* biomarkers. *Chemosphere.* 199, 427-434. <https://doi.org/10.1016/j.chemosphere.2018.02.050>

Kováčik, J., Babula, P., Hedbavny, J., 2017. Comparison of vascular and non-vascular aquatic plant as indicators of cadmium toxicity. *Chemosphere.* 180, 86-92. <https://doi.org/10.1016/j.chemosphere.2017.04.002>

Mittler, R., 2002. Oxidative stress, antioxidants and stress tolerance. *Trends Plant Sci.* 7, 405-410. [https://doi.org/10.1016/S1360-1385\(02\)02312-9](https://doi.org/10.1016/S1360-1385(02)02312-9)

Mittler, R., Vanderauwera, S., Gollery, M., Breusegem, F.V., 2004. Reactive oxygen gene network of plants. *Trends Plant Sci.* 9, 490-498. <https://doi.org/10.1016/j.tplants.2004.08.009>

Møller, I.M., 2001. Plant mitochondria and oxidative stress: electron transport, NADPH turnover, and metabolism of reactive oxygen species. *Annu. Rev. Plant Phys.* 52, 561-591. <https://doi.org/10.1146/annurev.arplant.52.1.561>

Mubarakshina, M.M., Ivanov, B.N., Naydov, I.A., Hillier, W., Badger, M.R., Krieger-Liszkay, A., 2010. Production and diffusion of chloroplastic H₂O₂ and its implication to signalling. *J. Exp. Bot.* 61(13), 3577-3587. <https://doi.org/10.1093/jxb/erq171>

Mullineaux, P.M., Exposito-Rodriguez, M., Laissue, P.P., Smirnov, N., 2018. ROS-dependent signalling pathways in plants and algae exposed to high light: Comparisons with other eukaryotes. *Free Radical Biol. Med.* 122, 52-64.

<https://doi.org/10.1016/j.freeradbiomed.2018.01.033>

Murashige, T., Skoog, F., 1962. A revised medium for rapid growth and bioassays with tobacco tissue cultures. *Physiol Plant.* 15, 472-497. <https://doi.org/10.1111/j.1399-3054.1962.tb08052.x>

Nakano, Y., Asada, K., 1981. Hydrogen peroxide is scavenged by ascorbate-specific peroxidase in spinach chloroplasts. *Plant Cell Physiol.* 22, 867-880.

<https://doi.org/10.1093/oxfordjournals.pcp.a076232>

Newete, S.W., Byrne, M.J., 2016. The capacity of aquatic macrophytes for phytoremediation and their disposal with specific reference to water hyacinth. *Environ. Sci. Pollut. Res.* 23, 10630-10643. <https://doi.org/10.1007/s11356-016-6329-6>

Nimptsch, J., Wunderlin, D.A., Dollan, A., Pflugmacher, S., 2005. Antioxidant and biotransformation enzymes in *Myriophyllum quitense* as biomarkers of heavy metal exposure and eutrophication in Suquía River basin (Córdoba, Argentina). *Chemosphere.* 61(2), 147-157. <https://doi.org/10.1016/j.chemosphere.2005.02.079>.

Pätsikkä, E., Kairavuo, M., Šeršen, F., Aro, E.M., Tyystjärvi, E., 2002. Excess copper predisposes photosystem II to photoinhibition *in vivo* by outcompeting iron and causing decrease in leaf chlorophyll. *Plant Physiol.* 129(3), 1359-1367.

<https://doi.org/10.1104/pp.004788>

Pilon, M., Abdel-Ghany S.E., Cohu, C.M., Gogolin, K.A., Ye, H., 2006. Copper cofactor delivery in plant cells. *Curr. Opin. Plant Biol.* 9(3), 256-263.

<https://doi.org/10.1016/j.pbi.2006.03.007>

Pilon, M., Ravet, K., Tapken, W., 2011. The biogenesis and physiological function of chloroplast superoxide dismutases. *Biochim. Biophys. Acta – Bioenergetics*. 1807(8), 989-998. <https://doi.org/10.1016/j.bbabi.2010.11.002>

Queval, G., Issakidis- Bourguet, E., Hoerberichts, F. A., Vandorpe, M., Gakière, B., Vanacker, H., Miginiac- Maslow, M., Van Breusegem, F., Noctor, G., 2007. Conditional oxidative stress responses in the Arabidopsis photorespiratory mutant *cat2* demonstrate that redox state is a key modulator of daylength- dependent gene expression, and define photoperiod as a crucial factor in the regulation of H₂O₂- induced cell death. *Plant J.* 52, 640-657. <https://doi.org/10.1111/j.1365-313X.2007.03263.x>

Ranieri, A., Castagna, A., Baldan, B., Soldatini, G.F., 2001. Iron deficiency differently affects peroxidase isoforms in sunflower. *J. Exp. Bot.* 52, 25-35. <https://doi.org/10.1093/jexbot/52.354.25>

Rausch, T., Gromes, R., Liedschulte, V., Müller, I., Bogs, J., Galovic, V., Wachter, A., 2007. Novel Insight into the Regulation of GSH Biosynthesis in Higher Plants. *Plant Biol.* 9, 565-572. <https://doi.org/10.1055/s-2007-965580>

Romero-Puertas, M.C., Rodríguez-Serrano, M., Corpas, F.J., Gómez, M., Del Río, L.A., Sandalio, L.M., 2004. Cadmium induced subcellular accumulation of O₂⁻ and H₂O₂ in pea leaves. *Plant Cell Environ.* 27, 1122-1134. <https://doi.org/10.1111/j.1365-3040.2004.01217.x>

Romero-Puertas, M.C., Terrón-Camero, L.C., Peláez-Vico, M.A., Olmedilla, A., Sandalio, L.M., 2019. Reactive oxygen and nitrogen species as key indicators of plant responses to Cd stress. *Environ. Experim. Bot.*, 161, 107-119. <https://doi.org/10.1016/j.envexpbot.2018.10.012>

Srivastava, S., Mishra, S., Tripathi, R.D., Dwivedi, S., Gupta, D.K., 2006. Copper-induced oxidative stress and responses of antioxidants and phytochelatins in *Hydrilla*

verticillata (L.f.) Royle. *Aquat. Toxicol.* 80, 405-415.

<https://doi.org/10.1016/j.aquatox.2006.10.006>

Su, T., Wang, P., Li, H., Zhao, Y., Lu, Y., Dai, P., Ren, T., Wang, X., Li, X., Shao, Q., Zhao, D., Zhao, Y., Ma, C., 2018. The Arabidopsis catalase triple mutant reveals important roles of catalases and peroxisome-derived signaling in plant development. *J. Integr. Plant Biol.* 60(7), 591-607. <https://doi.org/10.1111/jipb.12649>

Tewari, R., Kumar, P., Sharma, P., 2005. Signs of oxidative stress in the chlorotic leaves of iron starved plants. *Plant Sci.* 169, 1037-1045.

<https://doi.org/10.1016/j.plantsci.2005.06.006>

Thomas, G., Stärk, H-J., Wellenreuther, G., Dickinson, B.C., Küpper, H., 2013. Effects of nanomolar copper on water plants—Comparison of biochemical and biophysical mechanisms of deficiency and sublethal toxicity under environmentally relevant conditions. *Aquat. Toxicol.* 140–141, 27-36. <https://doi.org/10.1016/j.aquatox.2013.05.008>

Thomas, G., Andresen, E., Mattusch, J., Hubáček, T., Küpper, H., 2016. Deficiency and toxicity of nanomolar copper in low irradiance—A physiological and metalloproteomic study in the aquatic plant *Ceratophyllum demersum*, *Aquat.Toxicol.* 177, 226-236.

<https://doi.org/10.1016/j.aquatox.2016.05.016>

Toppi, L.S.D., Vurro, E., Rossi, L., Marabottini, R., Musetti, R., Careri, M., Maffini, M., Mucchino, C., Corradini, C., Badiani, M., 2007. Different compensatory mechanisms in two metal-accumulating aquatic macrophytes exposed to acute cadmium stress in outdoor artificial lakes. *Chemosphere*, 68(4), 769-780.

<https://doi.org/10.1016/j.chemosphere.2006.12.092>

Upadhyay, R.K., Panda, S.K., 2009. Copper-induced growth inhibition, oxidative stress and ultrastructural alterations in freshly grown water lettuce (*Pistia stratiotes* L.). *C. R. Biol.* 332(7), 623-632. <https://doi.org/10.1016/j.crv.2009.03.001>

Wawrzyński, A., Kopera, E., Wawrzyńska, A., Kamińska, J., Bal, W., Sirko, A., 2006. Effects of simultaneous expression of heterologous genes involved in phytochelatins biosynthesis on thiol content and cadmium accumulation in tobacco plants. *J. Exp. Bot.* 57(10), 2173–2182. <https://doi.org/10.1093/jxb/erj176>

Yruela, I., 2005. Copper in plants. *Braz. J. Plant Physiol.* 17(1), 145-156. <http://dx.doi.org/10.1590/S1677-04202005000100012>

Zhuang, K., Shi, D., Hu, Z., Xu, F., Chen, Y., Shen, Z., 2019. Subcellular accumulation and source of $O_2^{\bullet-}$ and H_2O_2 in submerged plant *Hydrilla verticillata* (L.f.) Royle under NH_4^+ -N stress condition. *Aquat. Toxicol.*, 207, 1-12. <https://doi.org/10.1016/j.aquatox.2018.11.011>

FIGURES

Fig. 1: Simplified representation of the activity profiles obtained for each antioxidant enzyme and metal (copper or cadmium). The curves correspond to the polynomial trendlines (6th-order) of the activity profiles presented in Supplementary Figs. 1-4 (for each sampling date, three technical replicates based on three independent clones ground together, see Sections 2.3 and 2.4). These "smoothed curves" allow detecting the most significant fluctuations for each metal concentration throughout the 27 days of the assay. *APX* (*ascorbate peroxidase*), *CAT* (*catalase*), *GSH-Px* (*glutathione peroxidase*) and *SOD* (*superoxide dismutase*).

Journal Pre-proof

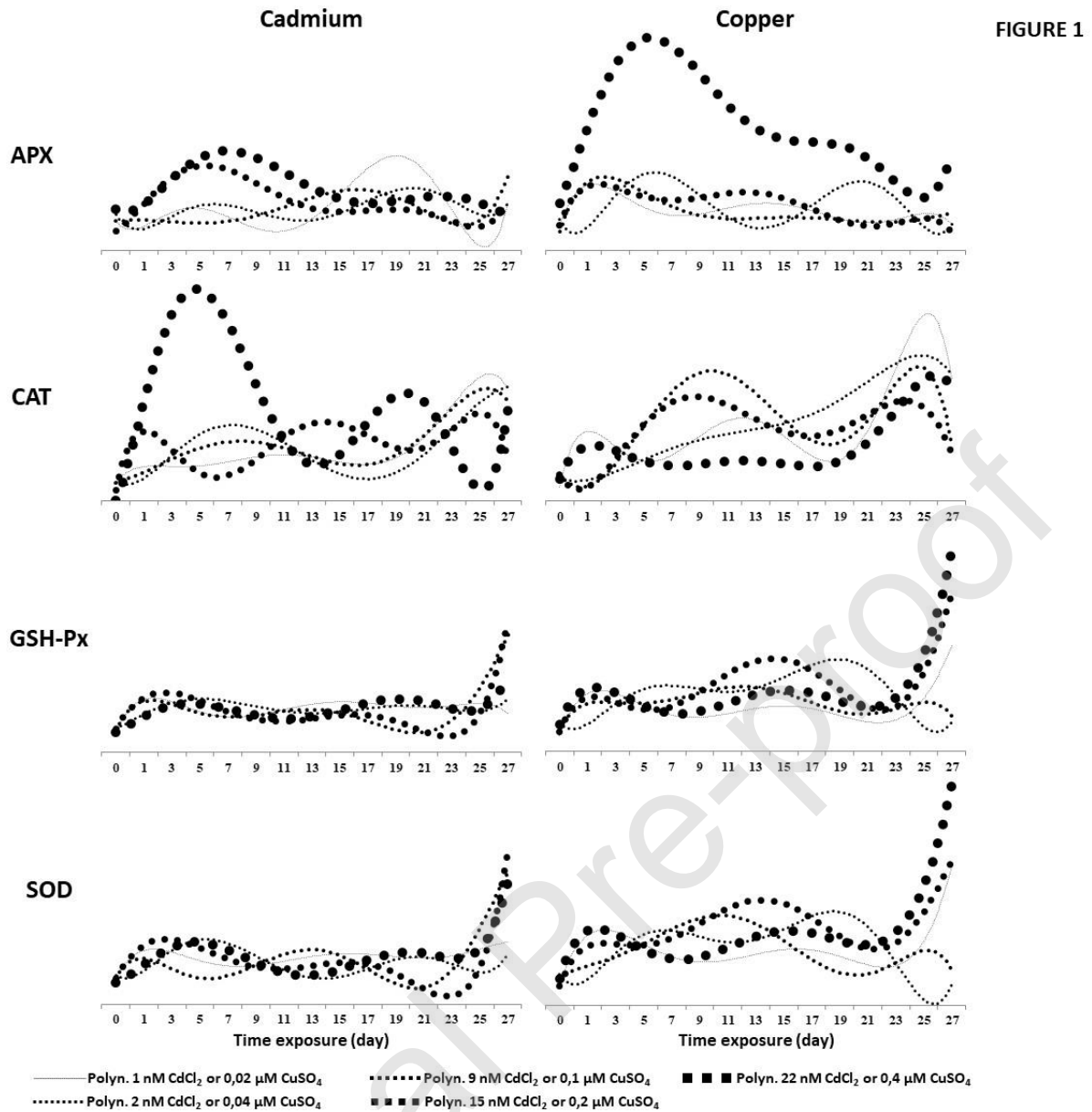


Fig. 2: Dendrogram of the Hierarchical Cluster Analysis (HCA) obtained from the activity profiles of the **ascorbate peroxidase (APX)**. This cluster analysis method was performed on raw data corresponding to enzyme activity measured at regular intervals during the 27 days of watermilfoil cultures, supplemented by cadmium (A) or copper (B) at different concentrations. Each detected clade is denoted by a colored square.

FIGURE 2

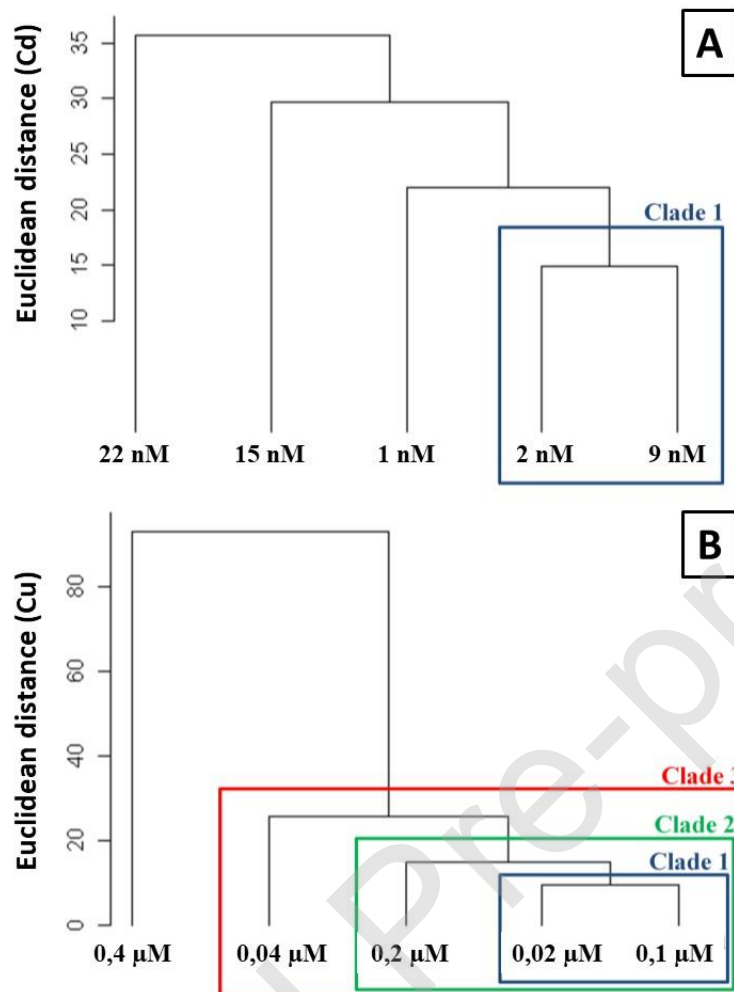


Fig. 3: Dendrogram of the Hierarchical Cluster Analysis (HCA) obtained from the activity profiles of the **catalase (CAT)**. This cluster analysis method was performed on raw data corresponding to enzyme activity measured at regular intervals during the 27 days of watermilfoil cultures, supplemented by cadmium (A) or copper (B) at different concentrations. Each detected clade is denoted by a colored square.

FIGURE 3

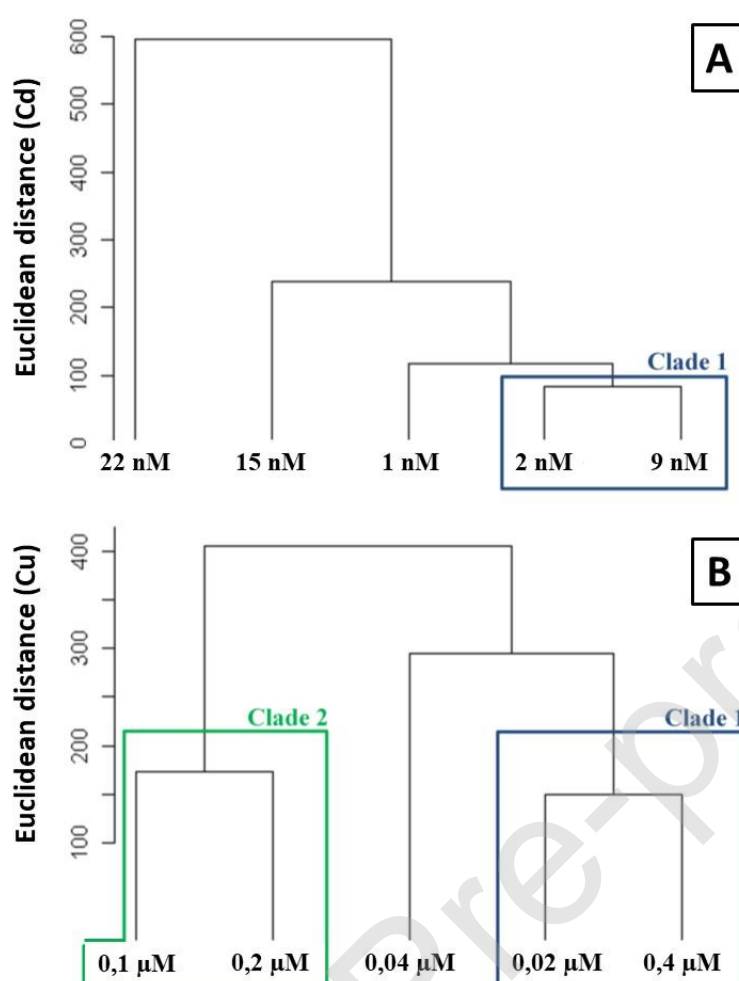


Fig. 4: Dendrogram of the Hierarchical Cluster Analysis (HCA) obtained from the activity profiles of the **glutathione peroxidase (GSH-Px)**. This cluster analysis method was performed on raw data corresponding to enzyme activity measured at regular intervals during the 27 days of watermilfoil cultures, supplemented by cadmium (A) or copper (B) at different concentrations. Each detected clade is denoted by a colored square.

FIGURE 4

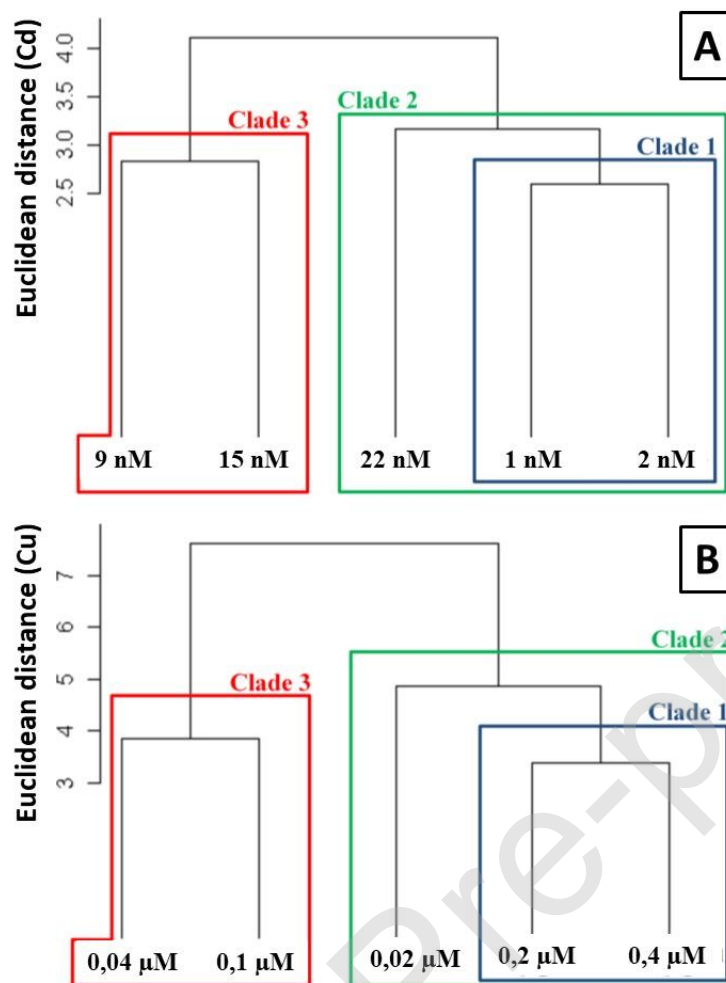
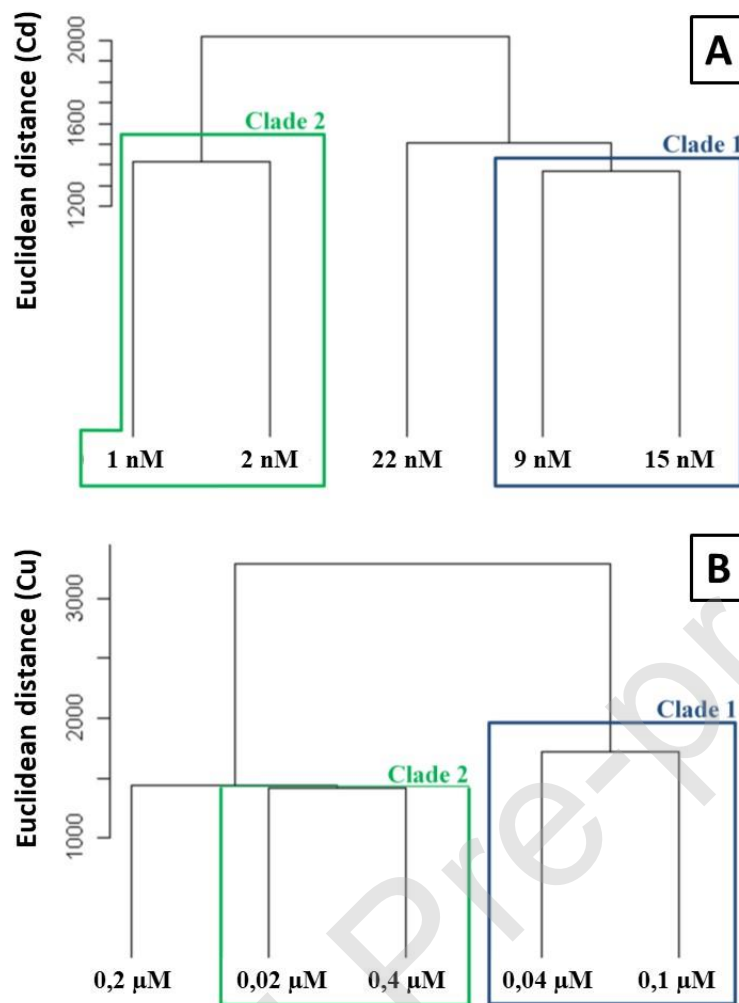


Fig. 5: Dendrogram of the Hierarchical Cluster Analysis (HCA) obtained from the activity profiles of the **superoxide dismutase (SOD)**. This cluster analysis method was performed on raw data corresponding to enzyme activity measured at regular intervals during the 27 days of watermilfoil cultures, supplemented by cadmium (A) or copper (B) at different concentrations. Each detected clade is denoted by a colored square.

FIGURE 5



SUPPLEMENTARY FIGURES

Fig. S1: Impact of different trace-metals concentrations on the **ascorbate-peroxidase (APX)** activity measured during 27 days in *M. alterniflorum*. Cadmium exposure corresponds to the gray histograms and copper exposure to the black histogram. Five concentrations of CuSO_4 or CdCl_2 were used and supplemented *in vitro* into the synthetic oligotrophic medium (the concentrations are defined in the top left-hand corner of each histogram). Each histogram bar reflects the mean of the three technical replicates. Error bars indicate standard deviations (the

biological sample at each sampling date corresponds to three independent clones ground together). Red arrows (↓) are placed on each observed peak.

Fig. S2: Impact of different trace-metals concentrations on the **catalase (CAT)** activity measured during 27 days in *M. alterniflorum*. Cadmium exposure corresponds to the gray histograms and copper exposure to the black histogram. Five concentrations of CuSO₄ or CdCl₂ were used and supplemented *in vitro* into the synthetic oligotrophic medium (the concentrations are defined in the top left-hand corner of each histogram). Each histogram bar reflects the mean of the three technical replicates. Error bars indicate standard deviations (the biological sample at each sampling date corresponds to three independent clones ground together). Red arrows (↓) are placed on each observed peak.

Fig. S3: Impact of different trace-metals concentrations on the **glutathione-peroxidase (GSH-Px)** activity measured during 27 days in *M. alterniflorum*. Cadmium exposure corresponds to the gray histograms and copper exposure to the black histogram. Five concentrations of CuSO₄ or CdCl₂ were used and supplemented *in vitro* into the synthetic oligotrophic medium (the concentrations are defined in the top left-hand corner of each histogram). Each histogram bar reflects the mean of the three technical replicates. Error bars indicate standard deviations (the biological sample at each sampling date corresponds to three independent clones ground together). Red arrows (↓) are placed on each observed peak.

Fig. S4: Impact of different trace-metals concentrations on the **superoxide-dismutase (SOD)** activity measured during 27 days in *M. alterniflorum*. Cadmium exposure corresponds to the gray histograms and copper exposure to the black histogram. Five concentrations of CuSO₄ or CdCl₂ were used and supplemented *in vitro* into the synthetic oligotrophic medium (the

concentrations are defined in the top left-hand corner of each histogram). Each histogram bar reflects the mean of the three technical replicates. Error bars indicate standard deviations (the biological sample at each sampling date corresponds to three independent clones ground together). Red arrows (↓) are placed on each observed peak.

Journal Pre-proof